IChemE
www.ingentaselect.com/titles/02638762.htm

0263–8762/03/$23.50+0.00

Trans IChemE, Vol 81, Part A, April 2003

COMPOSITION TRAJECTORIES FOR HETEROGENEOUS AZEOTROPIC DISTILLATION IN A BUBBLE-CAP TRAY COLUMN
Influence of Mass Transfer

P. A. M. SPRINGER, R. BAUR and R. KRISHNA

Department of Chemical Engineering, University of Amsterdam, Amsterdam, The Netherlands

The overall objective of this work is to examine the influence of interphase mass transfer on the composition trajectories in heterogeneous azeotropic distillation. Experiments were carried out in a bubble cap distillation column operated at total reflux with the systems: water–ethanol–cyclohexane and water–acetone–toluene. The experiments were carried out in regions of the composition space such that liquid–liquid phase splitting occurred on some of the trays. In order to model the composition trajectories, a rigorous non-equilibrium (NEQ) stage model is developed. The NEQ model incorporates the Maxwell–Stefan diffusion equations to describe the various intraphase transfers. The developed NEQ model is in good agreement with the experimental results for both experimental systems. In sharp contrast, an equilibrium (EQ) stage model fails even at the *qualitative* level to model the experiments. For example, for the water–ethanol–cyclohexane system the EQ model anticipates distillation boundary crossing when this does not take place in practice. For the water–acetone–toluene system the EQ model does not anticipate distillation boundary crossing when this phenomena is found in the experiments. It is concluded that for reliable design of azeotropic distillation columns we must take interphase mass transfer effects into account in a rigorous manner.

Keywords: heterogeneous azeotropic distillation; residue curve maps; Maxwell–Stefan equations; distillation boundary; nonequilibrium stage; equilibrium stage.

INTRODUCTION

The traditional method for simulating distillation tray columns is based on the *equilibrium* (EQ) stage model wherein the vapour leaving any stage is assumed to be in equilibrium with the liquid leaving that stage through the downcomer. In practice, the contact time between the vapour and liquid phases is not long enough for equilibrium to be established and Murphree (1925) was the first to provide a measure of approach to equilibrium by defining the *stage efficiency*:

$$E_i = \frac{y_{i,\mathrm{L}} - y_{i,\mathrm{E}}}{y_i^* - y_{i,\mathrm{E}}}; \quad i = 1, 2, \ldots, n \tag{1}$$

where the subscript i refers to species i in the n-component mixture, and the subscripts E and L refer to the entering and leaving streams on the stage; see Figure 1. The y_i^* represent the compositions of the vapour that would be in equilibrium with the liquid leaving the tray. The mole fractions add to unity:

$$\sum_{i=1}^{n} y_{i,\mathrm{L}} = 1; \quad \sum_{i=1}^{n} y_{i,\mathrm{E}} = 1; \quad \sum_{i=1}^{n} y_i^* = 1 \tag{2}$$

and, consequently, only $n-1$ of the Murphree stage efficiencies E_i are independent. For a binary mixture, $n = 2$, there is only one Murphree stage efficiency that is equal for components 1 and 2:

$$E_1 = \frac{y_{1,\mathrm{L}} - y_{1,\mathrm{E}}}{y_1^* - y_{1,\mathrm{E}}} = \frac{y_{2,\mathrm{L}} - y_{2,\mathrm{E}}}{y_2^* - y_{2,\mathrm{E}}} = E_2 \tag{3}$$

When the number of components n is three or more, there is no requirement that the Murphree efficiencies E_i be equal to one another:

$$E_1 \neq E_2 \neq E_3, \ldots, \neq E_n \tag{4}$$

There is a large body of experimental evidence for ternary distillation in the published literature to verify that component efficiencies are not equal to one another and that any of these efficiencies could vary from $-\infty$ to $+\infty$; see the comprehensive literature survey given in Chapter 13 of Taylor and Krishna (1993). Careful examination of the classic paper by Murphree (1925) reveals that he already appreciated equation (4) in 1925: 'For three-component mixtures the approach to equilibrium would not in general be equal for the two volatile components...'. It was only several decades later that procedures for calculation of the component Murphree efficiencies were developed by adopting the Maxwell–Stefan (M-S) formulation (Krishna and Wesselingh, 1997; Taylor and Krishna, 1993; Wesselingh and Krishna, 2000) to describe intraphase mass transport. In the M-S diffusion formulation, chemical potential gradients

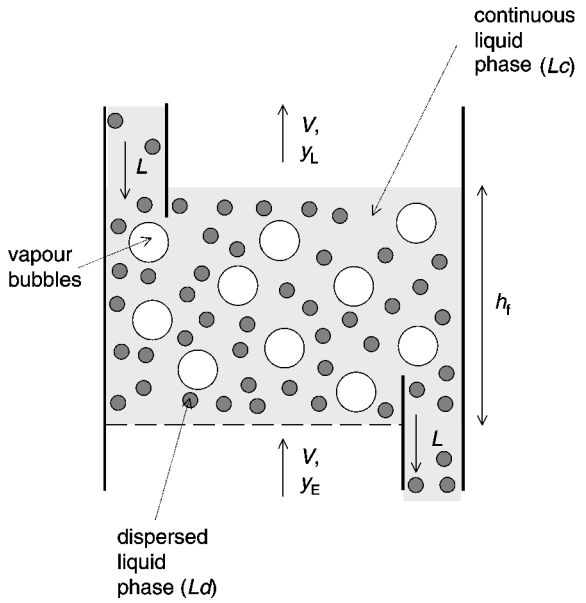

Figure 1. Schematic of the bubble froth regime on the tray with two liquid phases.

are used as the driving forces for diffusion and a linear relation is postulated between the driving forces and the fluxes in the form:

$$-\frac{x_i}{RT}\nabla\mu_i = \sum_{\substack{j=1\\ j\neq i}}^{n}\frac{x_jN_i - x_iN_j}{c_t\mathcal{D}_{ij}}; \quad i = 1, 2, \ldots, n \tag{5}$$

where x_i represent the mole fraction in the fluid phase under consideration; N_i are the molar fluxes; $\mathcal{D}_{ij}$ are the M-S diffusivities; and $\nabla\mu_i$ are the chemical potential gradients. It is of historical interest to note that Lewis and Chang (1928) were already aware of the usefulness of the Maxwell–Stefan formulation for modelling mass transfer on distillation trays.

Following the approach of Taylor and Krishna (1993), we can also write the M-S formulation in terms of the phase mass transfer coefficients κ_{ij}:

$$\sum_{j=1}^{n}\Gamma_{ij}\Delta x_j = \sum_{\substack{j=1\\ j\neq i}}^{n}\frac{x_jN_i - x_iN_j}{c_t\kappa_{ij}}; \quad i = 1, 2, \ldots, n-1 \tag{6}$$

where Δx_i represents the differences in composition between the bulk fluid phase and the interface. The Γ_{ij} represents thermodynamic correction factors

$$\Gamma_{ij} = \delta_{ij} + x_i\frac{\partial \ln\gamma_i}{\partial x_j}; \quad i, j = 1, 2, \ldots, n-1 \tag{7}$$

Equation (6) can be re-cast into $n-1$-dimensional matrix notation:

$$(N) = c_t[k][\Gamma](\Delta x) \tag{8}$$

where $[k]$ is the $(n-1)\times(n-1)$ dimensional square matrix of mass transfer coefficients. For a ternary system, the four elements of $[k]$ can be determined explicitly from the following set of equations (for derivations see Taylor and Krishna, 1993):

$$\begin{aligned} k_{11} &= \frac{\kappa_{13}[y_1\kappa_{23} + (1-y_1)\kappa_{12}]}{S}\\ k_{12} &= \frac{y_1\kappa_{23}(\kappa_{13} - \kappa_{12})}{S}\\ k_{21} &= \frac{y_2\kappa_{13}(\kappa_{23} - \kappa_{12})}{S}\\ k_{22} &= \frac{\kappa_{23}[y_2\kappa_{13} + (1-y_2)\kappa_{12}]}{S} \end{aligned} \tag{9}$$

where

$$S = y_1\kappa_{23} + y_2\kappa_{13} + y_3\kappa_{12} \tag{10}$$

Equations (8)–(10) show that flux of any species depends on the driving forces Δx_i of all the species present in the mixture. The extent of coupling depends *inter alia* on the *differences* in the transfer coefficients κ_{ij} of the binary pairs $i-j$ in the mixture in either fluid phase. For a mixture made up of components that are similar in molecular size, shape, polarity and hydrogen bonding characteristics, coupling effects are expected to be minimal and the component efficiencies are nearly equal to one another. This is the case, for example, for distillation of close boiling hydrocarbon mixtures. On the other hand for highly non-ideal mixtures of components with widely differing molar masses, coupling effects can expected to be very significant. The influence of diffusional coupling manifests itself in significant differences in the component E_i. For simulation of multicomponent distillation columns the M-S formulation has been incorporated into commercially available software packages such as RATEFRAC (marketed by Aspen Technology) and ChemSep (available through the CACHE corporation; see also www.chemsep.org). Such simulation models are usually called *rate-based* or *non-equilibrium* (NEQ) models to distinguish them from the classical approaches using EQ stage models.

Recently, Springer *et al.* (2002a–c) performed experiments in a distillation tray column with the *homogeneous* azeotropic systems water–ethanol–acetone, water–ethanol–methyl acetate, water–ethanol–methanol and water–ethanol–methanol–acetone to demonstrate that, as a consequence of differences in values of E_i, the composition trajectories in the column are significantly different from that predicted by the EQ stage model. More dramatically, they have shown that, for all the systems studied, distillation boundaries can be crossed when such crossing is disallowed by the EQ stage model. The work of Springer *et al.* (2002a–c) has underlined the need for rigorous NEQ models in simulation and design.

In the present communication we focus attention on *heterogeneous* azeotropic systems, i.e. systems that exhibit liquid–liquid phase splitting on at least some of the trays. Heterogeneous azeotropic distillation is widely encountered in the process industries (Doherty and Malone, 2001), for example in the production of dehydrated alcohol. Published simulation models for distillation tray columns with two-liquid phases include the EQ stage model (Block and Hegner, 1976), EQ stage model with Murphree stage efficiencies (Ross and Seider, 1981), and the NEQ stage model (Eckert and Vanek, 2001) in which the two-liquid phases are assumed to be in thermodynamic equilibrium.

Table 1. NRTL parameters for binary mixtures at 101.3 kPa, taken from Gmehling and Onken (1977). These parameters are used along with $G_{ij} = \exp(-\alpha_{ij}\tau_{ij})$ and $\tau_{ij} = B_{ij}/T$.

Component i	Component j	B_{ij} (K)	B_{ji} (K)	α_{ij}
Water	Ethanol	557.48	29.09	0.348
Water	Cyclohexane	4422.3	1688.3	0.212
Ethanol	Cyclohexane	440.61	717.68	0.463
Water	Acetone	653.89	377.58	0.586
Water	Toluene	2160.8	2839.4	0.200
Acetone	Toluene	−124.77	366.1	0.295

The experimental work of Cairns and Furzer (1990a–c) has shown that Murphree efficiencies E_i in three-phase distillation show strong variations from tray to tray and are also extremely sensitive to the choice of the thermodynamic model used for calculation of phase equilibria. Müller *et al.* (Müller and Marquardt, 1997; Müller *et al.*, 1997) have demonstrated the possibility of multiple steady states during distillation of water–ethanol–cyclohexane in a eight-stage bubble cap distillation column. Interestingly, Müller *et al.* (1997) concluded that the experimentally measured composition trajectories could be simulated with an EQ stage model with *equal* component efficiencies for all components in the mixture.

Our major objective is to investigate the influence of mass transfer on the composition trajectories in *heterogeneous* azeotropic distillation in order to check whether unequal component efficiencies E_i can lead to *qualitatively* different results from EQ stage models as was concluded earlier for *homogeneous* azeotropic distillation (Springer *et al.*, 2002a–c). Towards this end, we performed experiments with two systems: (a) water–ethanol–cyclohexane, and (b) water–acetone–toluene in a bubble-cap tray distillation column. The residue curve maps for these systems, calculated with NRTL parameters (Gmehling and Onken, 1977) listed in Table 1, are shown respectively in Figure 2(a) and (b); these residue curves and distillation boundaries take account of vapour–liquid–liquid equilibria. The grey shaded areas in Figure 2 indicate the region in which liquid–liquid phase splitting occurs. The water–ethanol–cyclohexane system shows a minimum boiling heterogeneous ternary azeotrope to which three distillation boundaries converge. The three distillation boundaries start at three different saddle points: (1) water–cyclohexane heterogeneous azeotrope; (2) water–ethanol azeotrope; and (3) ethanol–cyclohexane azeotrope. The water–acetone–toluene system shows one minimum boiling heterogeneous azeotrope between water and toluene and a straight distillation boundary connecting the azeotrope with pure acetone, see Figure 2(b).

EXPERIMENTAL SET-UP

The experiments were carried out in a laboratory-scale distillation column supplied by Schott Nederland B.V.; see Figure 3. The double-layered glass column with vacuum between the inner and outer shell contains a total condenser (stage 1), a partial reboiler (stage 12) and 10 bubble cap trays (stages 2 to 11) for which the dimensions are detailed in Table 2 and pictured in Figure 3. The distillation column is divided into two sets of five bubble cap trays by an intersection at which a continuous feed can be introduced to the column. Product streams can be tapped automatically from the condenser and manually from the reboiler. The glass distillation column has several small openings of 10 mm in diameter, which are sealed with Teflon-coated septa. These opening enable liquid and vapour samples to be withdrawn by means of a syringe. The column has a total height of 2160 mm and a 50 mm inner diameter.

The reboiler is placed in a heating mantle, which is connected to a PC provided with the required software (Honeywell: Windows NT Workstation 4.0; FIX MMI V 6.15/75-I/O-points runtime; OPTO CONTROL rel. 2.2a). By means of the PC, the reboiler temperature can be controlled as well as the feed and product flows. Furthermore it provides an automatic safety shut-down in case the column reboiler accidentally dries up. The condenser is connected

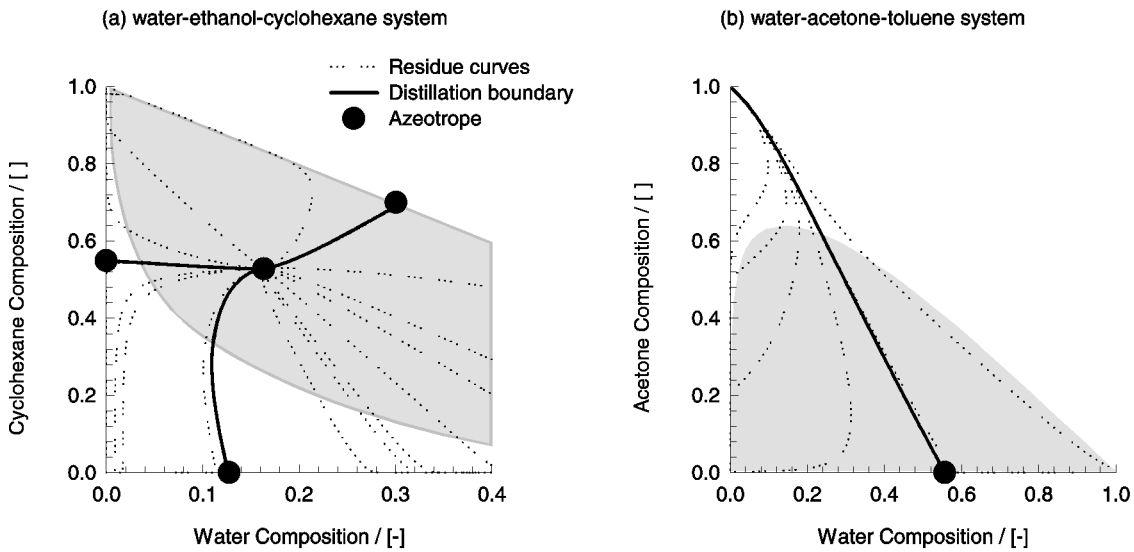

Figure 2. (a) Residue curve map for the water (1)–ethanol (2)–cyclohexane (3) system. (b) residue curve map for the water (1)–acetone (2)–toluene (3) system. The grey shaded areas represent the region in which liquid–liquid phase splitting occurs.

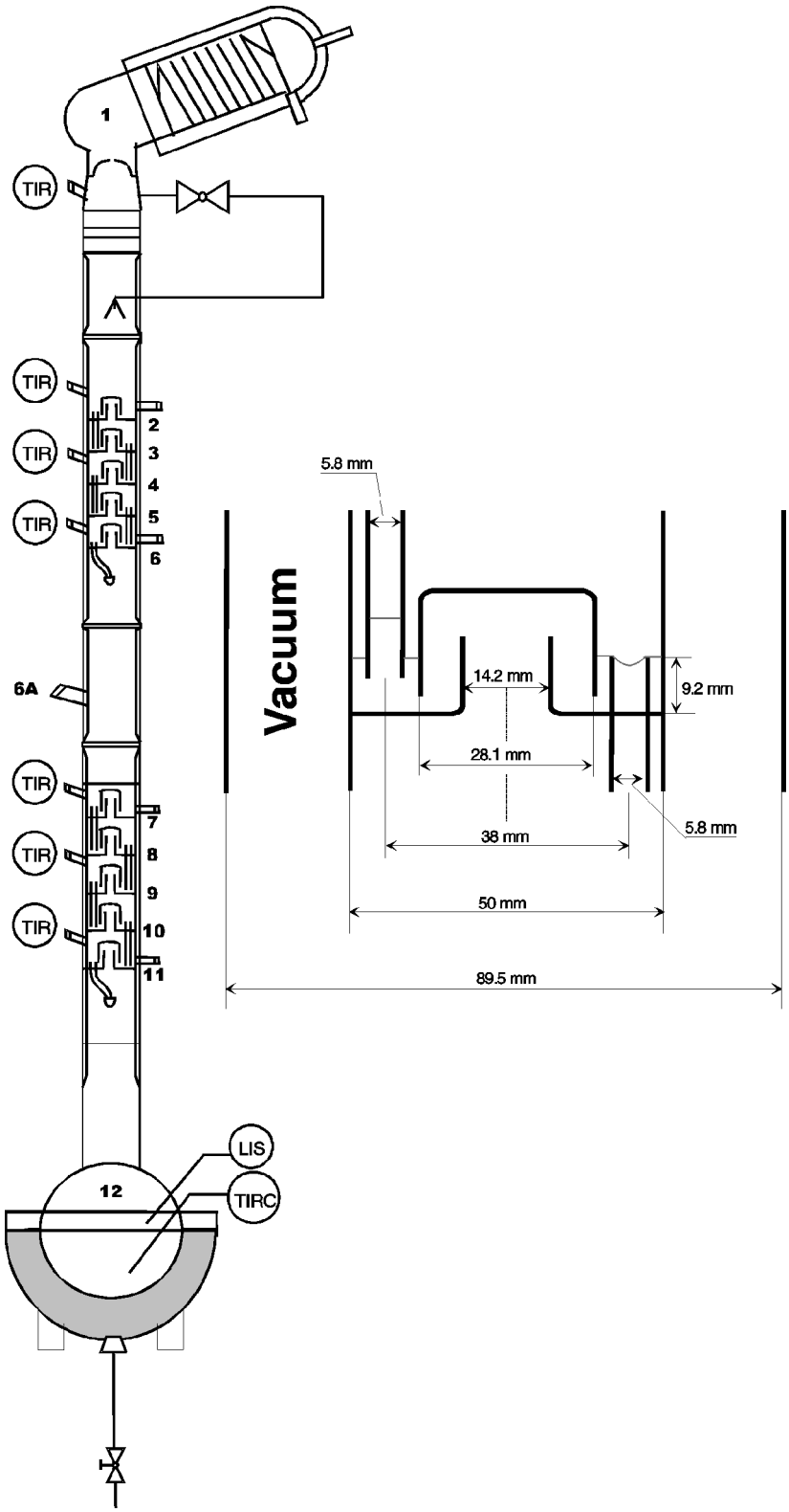

Figure 3. Schematic of laboratory-scale distillation column. Includes total condenser (1), partial reboiler (12), 10 bubble cap trays (2–11) and 13 draw-off faucets, nine for vapour samples (V) and four for liquid samples (L). (b) Details of bubble cap.

with a water tap, which supplies cooling water to the glass cooling tubes inside the condenser.

Experiments under total reflux conditions and atmospheric pressure were carried out with the systems water–ethanol–cyclohexane and water–acetone–toluene. For any given experiment, eight vapour and four liquid samples were taken from several stages (the sampling points are shown in Figure 3) and the temperature profile was measured with PT 100 sensors. Each sample volume was intentionally kept small (100 μL) to prevent changes in the composition profile

Table 2. Bubble cap tray design of the laboratory-scale distillation column.

Column diameter	50 mm	Hole pitch	14.2 mm
Tray spacing	46.2 mm	Cap diameter	28.1 mm
Number of flow passes	1	Skirt clearance	3 mm
Liquid flow path length	30.8 mm	Slot height	5 mm
Downcomer clearance	3.9 mm	Active area (of total area)	97.30%
Deck thickness	3 mm	Total hole area (of total area)	8.27%
Hole diameter	14.2 mm	Downcomer area (of total area)	1.35%
Weir type	Circular	Slot area	221 mm^2
Weir length	18.2 mm	Riser area	158 mm^2
Weir height	9.2 mm	Annular area	462 mm^2
Weir diameter	5.8 mm		

during the entire experiment. The samples were first dissolved into a reference solvent, consisting for the water–ethanol–cyclohexane system of 1 vol% *n*-propanol in 99 vol% acetone and for the water–acetone–toluene system of 1 vol% *n*-propanol in 99 vol% ethanol, before injection into the gas chromatograph (GC; type GC8000-Top with pressure/flow control) by means of an autosampler (type AS800). The channel inside the GC is made of stainless steel and has a total length of 1 m and 0.3175 mm diameter. The carrier gas used was helium because of its high thermal conductivity and chemical inertness. By analysing samples of pre-prepared, known compositions, the GC was carefully calibrated. More detailed descriptions of the experimental set-up, measurement technique, GC analysis and composition determination, including pictures of the column and bubble cap trays, are available on our web site: http://ct-cr4.chem.uva.nl/distillation/.

NEQ MODEL DEVELOPMENT

Before discussing the experimental results we extend the NEQ model developed earlier (Springer *et al.*, 2002a–c) in order to cater for liquid–liquid phase splitting on some or all of the trays. Visual observations of tray operation clearly showed which stages were still in the homogeneous region and which stages entered the heterogeneous region. The appearance of two liquids on a stage was visually indicated by a 'milky' emulsion, consisting of a continuous phase (phase Lc) in which a second liquid phase (phase Ld) was dispersed, as pictured in Figure 1. Our experimental results, to be discussed below, were conducted in composition regions poorer in water, and from consideration of the phase flows we concluded that the continuous liquid phase in the trays exhibiting phase splitting, in all experiments for both systems, was the 'organic' phase and the dispersed phase was the 'aqueous' phase. We therefore have to reckon with two interphase transfer processes: (1) dispersed aqueous phase (Ld) to continuous organic phase; (Lc) and (2) continuous organic liquid phase (Lc) to vapour (V). These transfer processes are pictured in Figure 4.

All our experiments were carried out in the bubbly froth regime. We assumed the bubbles to be of uniform size, having a diameter d_b. In this context reference must be made to the paper by Mehlhorn *et al.* (1996), who show that a two-bubble class model would be more appropriate; our approach of using an effective bubble diameter must be viewed as a first approximation. For the trays on which we have liquid–liquid phase splitting the liquid droplets are also assumed to be uniform in size, having a diameter d_d. Examination of the liquid–liquid emulsion phase under a microscope showed the aqueous phase droplet sizes to have diameters in the 10–30 μm range. In order to quantify the transfer processes, pictured in Figure 4, we extend the treatment in earlier publications by Taylor, Krishna and others (Baur *et al.*, 1999; Krishna and Wesselingh, 1997; Krishnamurthy and Taylor, 1985a–c; Springer *et al.*, 2002a–c; Taylor *et al.*, 1994; Taylor and Krishna, 1993; Wesselingh and Krishna, 2000) to three-phase dispersions. There are four transport resistances to reckon with. The transfer coefficients inside the rigid bubbles and within the aqueous phase drops can be estimated from taking the corresponding Sherwood numbers to equal $2\pi^2/3$ by extending the ideas of Springer *et al.* (2002a–c). For estimating the transfer coefficients in the continuous organic liquid phase surrounding the droplets we take a conservative estimate of $Sh = 2$. The estimation of the transfer coefficients in the continuous liquid phase surrounding the bubble follows the penetration model:

$$\kappa_{ij}^{\mathrm{Lc,b}} = 2\sqrt{\frac{Đ_{ij}^{\mathrm{Lc}}}{\pi t_b}} \tag{11}$$

where the contact time of the continuous liquid phase with gas bubbles, t_b is given by:

$$t_b = \frac{d_b}{V_b} \tag{12}$$

The bubble rise velocity V_b is estimated using the Mendelson equation (Krishna *et al.*, 1999; Mendelson, 1967), recommended by Krishna *et al.* (1999):

$$V_b = \sqrt{\frac{2\sigma^{\mathrm{Lc}}}{\rho^{\mathrm{Lc}} d_b} + \frac{g d_b}{2}} \tag{13}$$

The calculation method of the transfer coefficients κ_{ij} for all the four transfer resistances is summarized in Figure 4. The transfer coefficients are different for each of the three binary pairs 1–2, 1–2, and 2–3 in the ternary mixture. The binary pair κ_{ij} is obtained by substituting the appropriate binary pair M-S diffusivity, $Đ_{ij}$, in the fluid phase under consideration, into the relations presented in Figure 4. For a typical run WEC-8 for the water–ethanol–cyclohexane system, to be discussed in detail below, the various parameter values on stage 2 (tray below the condenser) have been listed in Table 3. The four transfer coefficient matrices $[k^{\mathrm{V}}]$, $[k^{\mathrm{Lc,b}}]$, $[k^{\mathrm{Lc,d}}]$ and $[k^{\mathrm{Ld}}]$ can then be calculated from equations (9) and (10) using the appropriate values of the bulk fluid phase compositions x_i and binary pair κ_{ij}.

The flux entering the vapour bubble can be expressed in terms of an overall matrix of mass transfer coefficients

$$(N) = c_t^{\mathrm{V}}[K^{\mathrm{OV}}](y^* - y) \tag{14}$$

where y_i^* is the composition of the vapour in equilibrium with the aqueous within the dispersed droplets. From the continuity relations for interphase mass transfer, the following

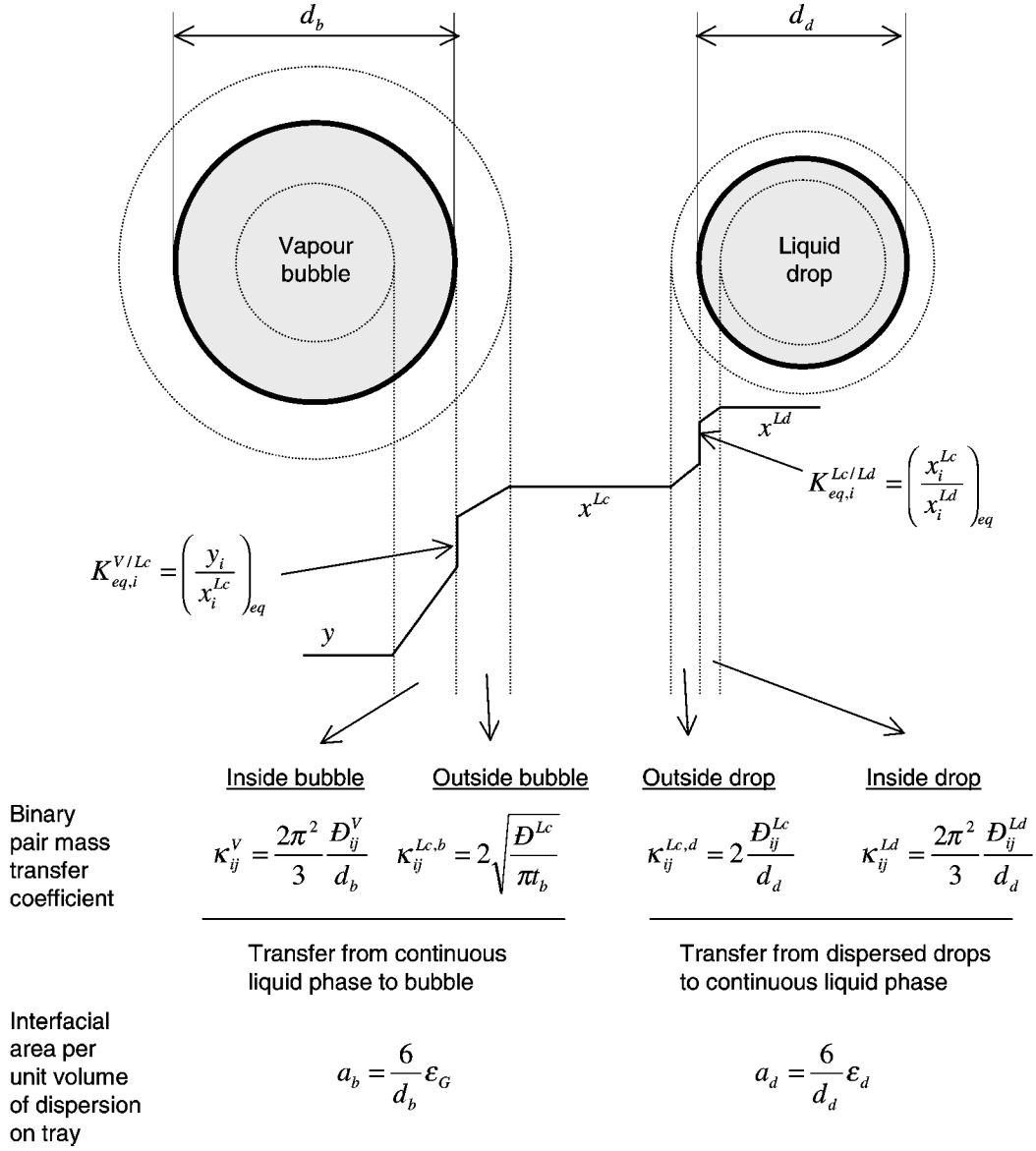

Figure 4. Schematic showing the four transfer resistances for three phase distillation.

expression can be derived for the overall transfer coefficient matrix $[K^{OV}]$:

$$[K^{OV}]^{-1} = [k^{V}]^{-1} + \frac{c_t^{V}}{c_t^{Lc}}[K_{eq}^{VLc}][k^{Lc,b}]^{-1} + \frac{c_t^{V}}{c_t^{Lc}}\frac{a_b}{a_d}[K_{eq}^{VLc}][k^{Lc,d}]^{-1} + \frac{c_t^{V}}{c_t^{Ld}}\frac{a_b}{a_d}[K_{eq}^{VLc}][K_{eq}^{LcLd}][k^{Ld}]^{-1} \quad (15)$$

The $[K_{eq}^{VLc}]$ and $[K_{eq}^{LcLd}]$ are diagonal K-value matrices with elements

$$K_{eq}^{VLc} = \left(\frac{y_i}{x_i^{Lc}}\right)_{eq}; \quad K_{eq}^{LcLd} = \left(\frac{x_i^{Lc}}{x_i^{Ld}}\right)_{eq}; \quad i = 1,2 \quad (16)$$

The K-values defined in equation (16) are used only for the estimation of the overall mass transfer coefficients following equation (15); for the estimation of the vapour–liquid–liquid equilibria use is made of the rigorous NRTL equations.

The values of the κ_{ij} in the liquid phases have the same order of magnitudes (see Table 3) and therefore the elements of matrices $[k^{Lc,b}]^{-1}$, $[k^{Lc,d}]^{-1}$ and $[k^{Ld}]^{-1}$ will be of the same order of magnitude. The contribution of the last two resistances on the right member of equation (15) will be negligible compared with the contributions of the first two terms because the ratios $c_t^{V}a_b/c_t^{Lc}a_d$ and $c_t^{V}a_b/c_t^{Ld}a_d$ have values of 3.5×10^{-5} and 1.9×10^{-5}, respectively, for the chosen values of the bubble diameter (2.5 mm) and drop diameter (10 μm). Put another way, the two liquid phases can be assumed to be in equilibrium with each other; this is the assumption made also by the Eckert and Vanek (2001) in the development of their NEQ model for three phase distillation. This also implies that the precise knowledge of the droplet diameter is unnecessary.

The next step in the model development is to integrate the flux expression for interphase transfer along the height of

Table 3. Physical and transport properties for stage 2 of run WEC-8 with the water (1)–ethanol (2)–cyclohexane (3) system presented in Figure 9; obtained by NEQ model simulations with a 2.5 mm bubble diameter and a droplet-size of the dispersed phase of 10 μm.

		i–j pair		
Parameter	Units	1–2 pair	1–3 pair	2–3 pair
$Đ_{ij}^{V}$	$10^{-5}\,m^2\,s$	1.981	1.275	0.639
$Đ_{ij}^{Lc}$	$10^{-9}\,m^2\,s$	5.364	6.964	3.517
$Đ_{ij}^{Ld}$	$10^{-9}\,m^2\,s$	4.224	2.955	2.017
ε_b			0.439	
ε_d			0.195	
d_b	mm		2.5	
d_d	μm		10.0	
V_b	$m\,s^{-1}$		0.190	
t_b	s		0.0132	
κ_{ij}^{V}	$mm\,s^{-1}$	52.1	33.5	16.8
$\kappa_{ij}^{Lc,b}$	$mm\,s^{-1}$	0.72	0.82	0.58
$\kappa_{ij}^{Lc,d}$	$mm\,s^{-1}$	1.1	1.4	0.7
$\kappa_{ij}^{Ld,d}$	$mm\,s^{-1}$	2.8	1.9	1.3
c_t^{V}	$mol\,m^{-3}$		0.036	
c_t^{Lc}	$mol\,m^{-3}$		9.33	
c_t^{Ld}	$mol\,m^{-3}$		17.7	
σ^{Lc}	$N\,m^{-1}$		0.022	
ρ^{Lc}	$kg\,m^{-3}$		746.5	
τ_V	s		0.0485	

dispersion on the tray. We assume that the bubbles rise through the liquid in a plug flow manner and that liquid phase is well mixed. The steady-state component molar balance for vapour flow through the froth on the tray for three-component distillation is given by the two-dimensional matrix relation

$$V_b \frac{d(y)}{dh} = [K^{OV}](y^* - y)\frac{6}{d_b} \tag{17}$$

where d_b is the diameter of the bubbles rising in the froth with a rise velocity V_b. Equation (17) can be re-written in terms of the overall number of transfer units for the vapour phase, $[NTU^{OV}]$:

$$\frac{d(y)}{d\xi} = [NTU^{OV}](y^* - y) \tag{18}$$

where $\xi = h/h_f$ is the dimensional distance along the froth and $[NTU^{OV}]$ is defined as:

$$[NTU^{OV}] = [K^{OV}]\frac{6}{d_b}\tau^{V} \tag{19}$$

where the vapour residence time is determined from

$$\tau^{V} = \frac{h_f}{V_b} \tag{20}$$

where h_f is the height of dispersion (froth). The height of the dispersion on the tray is taken to be the height of the downcomer tube above the tray floor, i.e. 9.2 mm as seen in Figure 3. This is a good approximation; any uncertainties in the value of h_f will be reflected in the choice of the bubble size. In the estimation of the bubble rise velocity the properties of the continuous organic phase (Lc) is used in equation (13).

Assuming that the $[NTU^{OV}]$ on a single stage is constant, equation (18) can be integrated using the boundary conditions

$$\begin{aligned} &\xi = 0 \text{ (inlet to tray):} \quad (y) = (y_E) \\ &\xi = 1 \text{ (outlet of tray):} \quad (y) = (y_L) \end{aligned} \tag{21}$$

to obtain the compositions leaving the distillation stage. Detailed derivations are available in Taylor and Krishna (1993):

$$(y^* - y_L) = \exp(-[NTU^{OV}])(y^* - y_E) \tag{22}$$

Introducing the matrix $[Q] \equiv \exp(-[NTU^{OV}])$, we can re-write equation (22) in the form

$$(y_L - y_E) = ([I] - [Q])(y^* - y_E) \tag{23}$$

where $[I]$ is the identity matrix. The limiting case of the EQ stage model is obtained when the NTU_{ij}^{OV} attain large values; $[Q]$ reduces in this case to the null matrix and the compositions leaving the tray (y_L) are equal to (y^*), in equilibrium with the liquid leaving the tray. Substituting equation (15) in equation (19) gives us the $[NTU^{OV}]$, required for calculation of the $[Q]$ matrix in equation (23). We follow the procedure of Kooijman and Taylor (1995) for implementation of equation (23) in the stage-to-stage calculation.

The material balance relations outlined above need to be solved along with the enthalpy balance relations. The required heat transfer coefficients in the vapour phase are calculated from the heat transfer analogue of the mass transfer equations.

The entire set of material and energy balance equations, along with the interphase mass and energy transfer rate relations are then incorporated into a rigorous stage-to-stage model as described in Chapter 14 of Taylor and Krishna (1993). The chapter contains more exhaustive detail of this model including sample calculations for binary and ternary mixtures.

SIMULATION STRATEGY

Simulations of the total reflux experimental runs were carried out using both the EQ stage model and the rigorous NEQ stage model developed above. The operating pressure for all experiments was 101.3 kPa and the ideal gas law was used. Activity coefficients were calculated using the NRTL interaction parameters, specified in Table 1, and the vapour pressures were calculated using the Antoine equations. The vapour phase was assumed to be thermodynamically ideal. The column consists of 12 stages, including the total condenser (stage 1) and partial reboiler (stage 12). The reflux flow rate ($0.003\,mol\,s^{-1}$) and the bottom flow rate ($0.0\,mol\,s^{-1}$) were used for specifying the column operations. Since the mass and heat transfer coefficients are independent of the internal flows, the composition and temperature profiles are not dependent on the precise value of the specified reflux flow rate.

Since the column is operated at total reflux, the reflux flow rate determined the inner flow rates of vapour and liquid phases on each stage. Simulation of total reflux operations is 'complicated' by the fact that there is no feed to the column at steady state. To overcome this problem we specify one of the experimentally determined compositions of the streams leaving or entering a stage as input parameter. The simulated composition profile of the total reflux run is forced to pass through this specified composi-

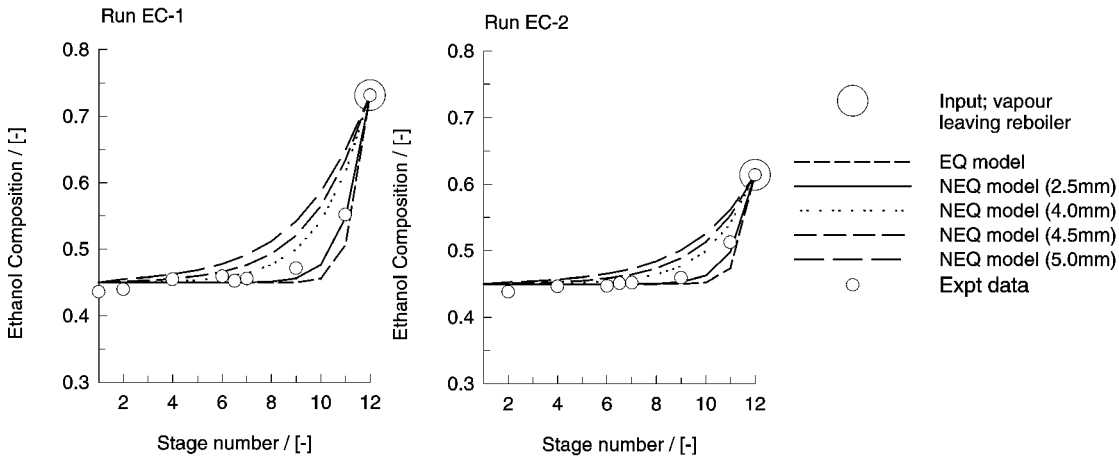

Figure 5. Experimental results (open circles for vapour samples) showing the column composition trajectories for the ethanol (1)–cyclohexane (2) binary system. Also shown are the simulation results showing the trajectories calculated by the NEQ stage model with different bubble diameters and the EQ stage model. The experimental vapour composition leaving the reboiler is specified in the simulations, denoted by the large open circle.

tion. The 'input' composition is indicated by the large open circle when comparing the experimental results with simulations in the figures to be discussed below. The entire set of equations system was solved numerically using the Newton's method (Krishnamurthy and Taylor, 1985a). The NEQ implementation is available in the software program *ChemSep*, developed by Taylor and others (Krishnamurthy and Taylor, 1985a–b; Taylor *et al.*, 1994; Taylor and Krishna, 1993). Detailed information on *ChemSep* are available in the recent book by Kooijman and Taylor (2001).

From the model development described above, we saw that the only unknown parameter is the bubble diameter d_b. Once this parameter is set the complete system of equations can be solved. To find out what the best fitting bubble diameter for the heterogeneous ternary azeotropic systems will be, we first performed a couple of experiments with the binary system ethanol (1)–cyclohexane (2). For this system, the simulations were carried out by specifying the vapour composition leaving the reboiler (stage 12). As we proceeded up the column we approached the azeotropic composition. Figure 5 shows that these binary experiments were best fitted with a 2.5 mm bubble diameter. With this information, we start the discussions of the experimental results for the two ternary heterogeneous azeotropic systems, along with simulation results.

EXPERIMENTS VS SIMULATIONS

The experimental results of the first system water (1)–ethanol (2)–cyclohexane (3) are subdivided into three different campaigns A, B and C, since the measured composition profiles are located in three different regions of the triangle composition space. The first set of three experiments, runs WEC-1, 2 and 3, are shown in Figure 6.

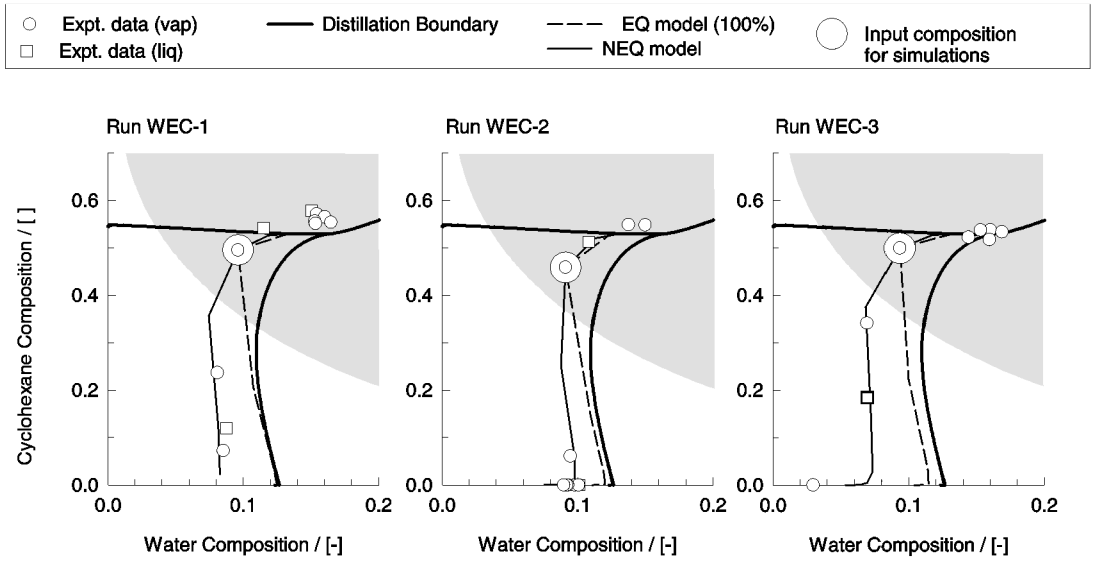

Figure 6. Experimental results (open circles for vapour samples and open squares for liquid samples) showing the column composition trajectories for the water (1)–ethanol (2)–cyclohexane (3) system for campaign A. Also shown are the simulation results showing the trajectories calculated by the EQ stage model and the NEQ stage model. The large open circles represent the experimental composition specified in the simulations. In the NEQ model simulations a bubble size $d_b = 2.5$ mm was chosen.

Besides nine vapour samples, four liquid samples of different stages are also plotted in one single graph because, at total reflux, the composition of the vapour leaving any given stage equals the composition of the liquid arriving at that stage from above for total reflux operation at steady state. In Figure 6 the vapour samples are denoted by open circles and the liquid samples by open squares. The large open circles represent the input composition in the simulations.

All the experimental results of campaign A show composition profiles that follow a trajectory from the ethanol corner towards the heterogeneous ternary azeotrope, see Figure 6. The simulation results obtained with the EQ stage model (100% efficiency) and the NEQ stage model with a 2.5 mm bubble diameter are also shown in the Figure 6. We note that the NEQ model in which mass transfer effect are included does a much better job of predicting the composition trajectory followed by the experiments. Another interesting point to note is that the experimental compositions of the column as we move down the column to the reboiler tend to move in the direction of pure ethanol. This is also the trend with the NEQ model. The EQ model (with 100% efficiency) predicts a different trend. Here the compositions as we move down the column have a tendency to become richer in water than in ethanol.

From the experimental data with the binary system ethanol–cyclohexane, we know that a 2.5 mm bubble diameter is the best fit value. For run WEC-2 we carried out simulations with the NEQ model for a range of bubble diameters; see the results in Figure 7. The value $d_b = 2.5$ mm matches the experiments quite closely. This is the case for campaigns A, B and C for the water–ethanol–cyclohexane system.

The results of campaign B, runs WEC 4–9 are presented in Figure 8. The experimental measured profiles in this campaign have their reboiler composition just to the left of the distillation boundary that connects the water–ethanol azeotrope to the heterogeneous ternary azeotrope. Proceeding up the column, the composition profile stays at the left of this boundary and ends up with a condenser composition in the heterogeneous ternary azeotrope, or close to it. In none of the experimental runs WEC 4–9 is boundary crossing observed. Also plotted in Figure 8 are the simulation results for the EQ (100% efficiency) and NEQ models. The NEQ model, with 2.5 mm bubble diameter, is able to simulate all the experimental runs very well. The EQ model, with 100% efficiency for each component, on the other hand is unable to match the experimental composition trajectories. For all the runs in campaign B, the EQ model predicts that the distillation boundary will be crossed and the compositions become richer in water as we proceed down the reboiler. Such boundary crossing is not disallowed and has been explained in detail by Levy *et al.* (1985). They state 'If the simple distillation boundary is curved, then the steady-state composition profile in a continuous distillation column cannot cross the boundary from the concave side but may cross the boundary from the convex side when moving from the product compositions inward'. No boundary crossing is observed experimentally.

In order to understand the qualitative differences between the EQ and NEQ models, let us examine run WEC-8 in some more detail. In Figure 9 the NEQ simulation results are presented for bubble sizes of 2.5, 3 and 4 mm. We note that, as for the results in campaign A, the best agreement with experiments is obtained with a bubble size of 2.5 mm. The component Murphree efficiencies for each component, calculated with the NEQ model (2.5 mm bubble size) is shown in Figure 10. We note that component efficiencies vary from tray to tray and are different for each component. The average efficiency for the whole column, for all three components, is around 80%. The differences in the component efficiencies are primarily to be ascribed to differences in the values of the vapour diffusivities, $Đ_{ij}^{V}$. The vapour phase diffusivities of the three binary pairs are estimated using the Fuller–Schettler–Giddings equation (Kooijman and Taylor, 2001; Poling *et al.*, 2000) and are listed in Table 3. As a consequence of the differences in the pair $Đ_{ij}^{V}$, the binary pair κ_{ij}^{V} are also different from one another. These differences lead to finite, large, off-diagonal elements in the matrix $[k^{V}]$, when calculated using equation (9). These

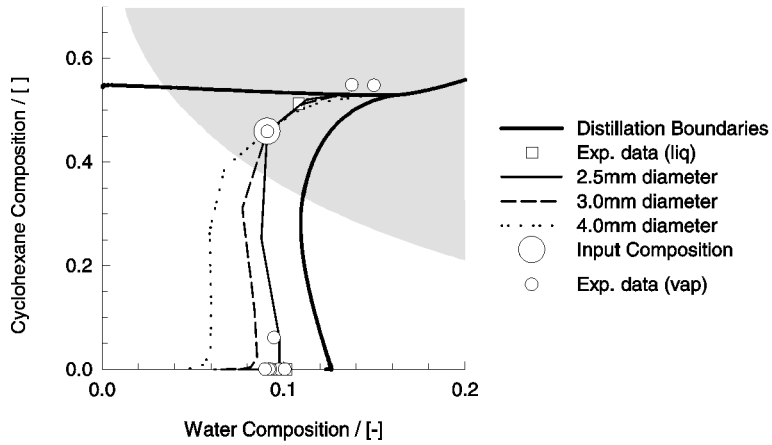

Figure 7. NEQ simulation results, with varying bubble diameters, compared with the experimental data (open circles for vapour samples and open squares for liquid samples) for run WEC-2 of campaign A.

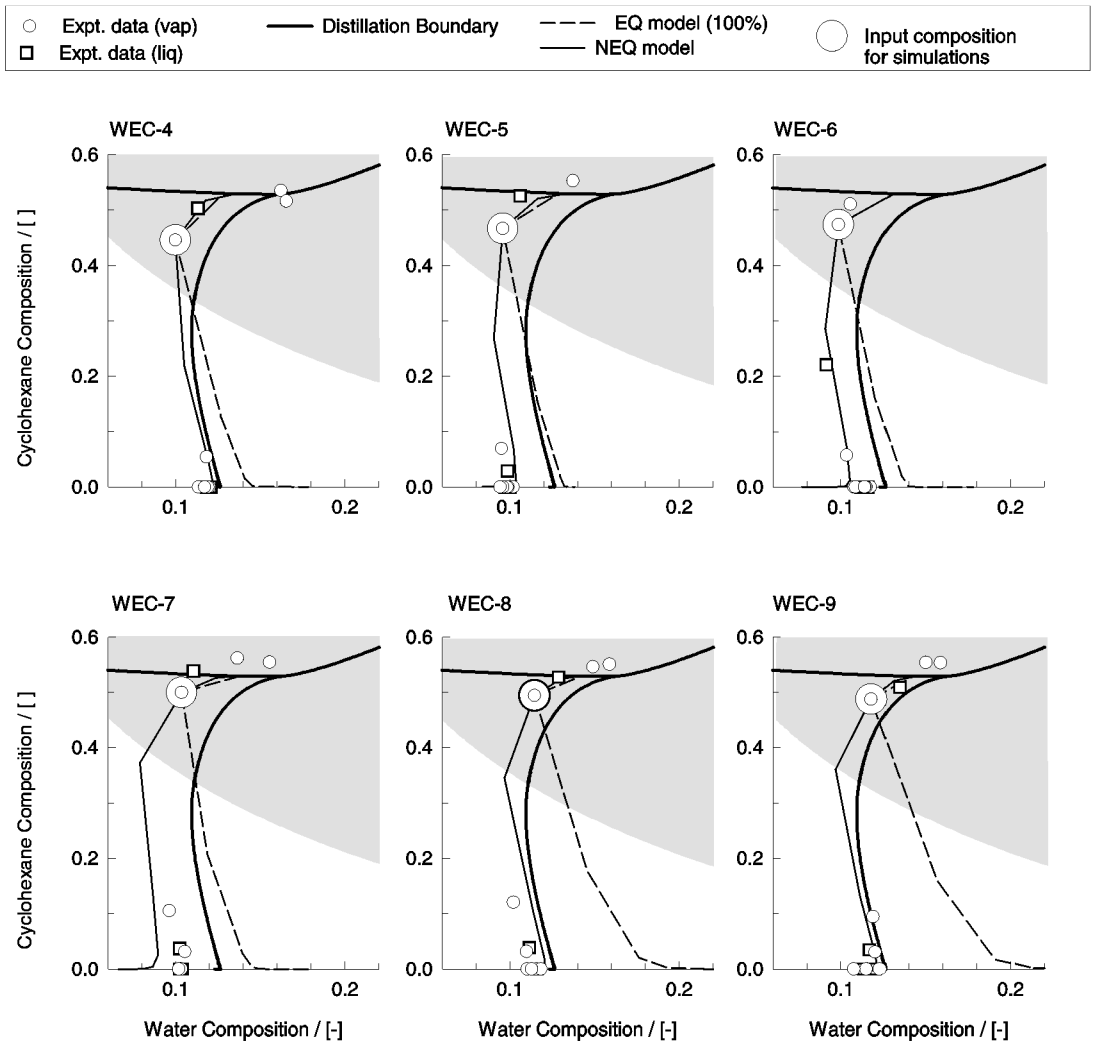

Figure 8. Experimental results (open circles for vapour samples and open squares for liquid samples) showing the column composition trajectories for the water (1)–ethanol (2)–cyclohexane (3) system for campaign B. Also shown are the simulation results showing the trajectories calculated by the EQ stage model and the NEQ stage model. The large open circles represent the experimental composition specified in the simulations. In all the NEQ model simulations a bubble size $d_b = 2.5$ mm was chosen.

off-diagonal elements are the primary cause of the differences in the component E_i.

In Figure 9(b) the EQ model simulation results are shown for two cases, with 100% and 80% efficiency for each component on all stages. Both the EQ models anticipate boundary crossing phenomena whereas no such crossing is found in practice. The inescapable conclusion to be drawn is that the assumption of equal component efficiency for each component in the mixture leads to erroneous results. This conclusion is in sharp contrast to that drawn by Müller *et al.* (1997); these authors concluded that the experimentally measured composition trajectories for the water–ethanol–cyclohexane system could be simulated with an EQ stage model with *equal* component efficiencies for all components in the mixture. This conclusion is clearly not valid for all regions of the composition space but is restricted to the some specific regions, as we shall see below.

Consider three experimental runs WEC-10, 11 and 12 of campaign C. In all three experiments boundary crossing is observed in the experiments; see Figure 11. This boundary crossing phenomena is anticipated by both NEQ and EQ models. To appreciate this fact let us consider the run WEC-12 in more detail. The NEQ simulation results for this run WEC-12 for various bubble sizes is shown in Figure 12(a). Again, the 2.5 mm bubble size gives the best agreement with the experimental results. The component efficiency for this run is 80%, when averaged over all trays for all three components. The simulation results with the EQ model taking all component efficiencies to be equal to either 80% or 100% are shown in Figure 12(b). The 80% EQ model simulations are practically indistinguishable from those of the complete NEQ model (2.5 mm bubble). This finding is in agreement with those of Müller *et al.* (1997). In this region of composition space of campaign C, the EQ model with equal component efficiencies is adequate to explain the composition trajectories.

Finally, let us consider the experimental composition trajectories in two runs WAT-1 and WAT-2 for the system water (1)–acetone (2)–toluene (3), for which the residue curve map is presented in Figure 2(b). In both runs the compositions get richer in acetone as we progress up the column towards the condenser. Proceeding down the

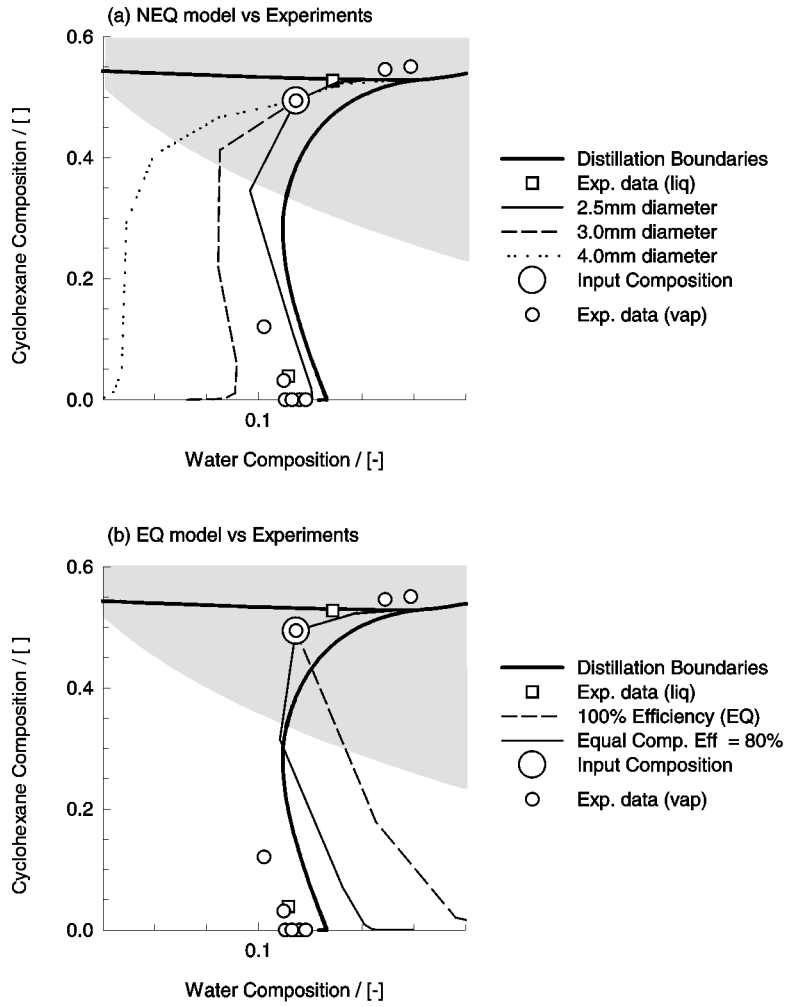

Figure 9. Simulation results compared with the experimental data (open circles for vapour samples and open squares for liquid samples) for run WEC-8 of campaign B. The large open circle is the specified input composition for the simulations. (a) The NEQ model, for varying bubble diameters is compared with experimental results. (b) The EQ model results with 100% and with 80% efficiency for all components are compared with experimental results.

column, the composition profile is just to the right of the straight distillation boundary. The trajectories suddenly move away from the water corner and cross the distillation boundary to finally end up in the toluene-rich corner of the liquid–liquid heterogeneous region. The point at which this sudden change in direction occurs just to the right of the distillation boundary has been used as starting point for the simulation with the EQ and NEQ stage model (denoted by the large open circle). It is clear that only the NEQ stage model (with 2.5 mm bubble size) with inclusion of mass transfer anticipates crossing of the distillation boundary to end up also with a reboiler composition richer in toluene. The EQ model fails at a qualitative level, since it predicts a reboiler composition of pure water; see Figure 13(a) and (b).

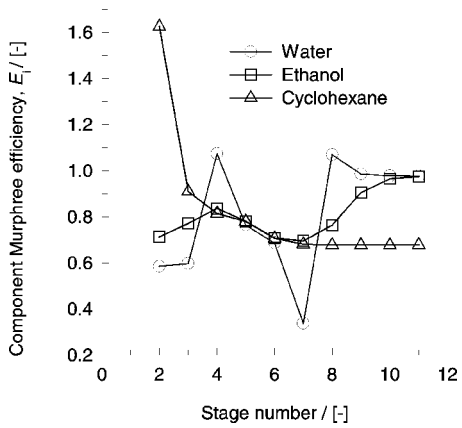

Figure 10. Component Murphree efficiencies along the column for run WEC-8 of campaign B, calculated by the NEQ stage model. In the NEQ model simulations a bubble size $d_b = 2.5$ mm was chosen.

CONCLUSIONS

The following major conclusions can be drawn from the work presented in this paper.

(1) For both water–ethanol–cyclohexane and water–acetone–toluene systems, the NEQ model is superior to the EQ model in its ability to predict the column composition trajectories.
(2) For the experimental runs in campaign C with the system water–ethanol–cyclohexane system (see Figures 11

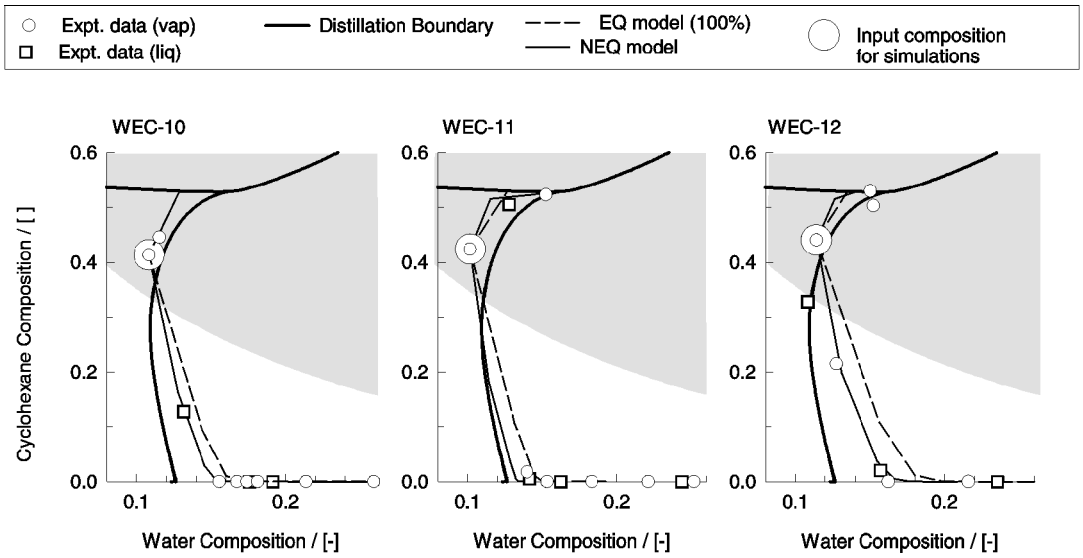

Figure 11. Experimental results for campaign C (open circles for vapour samples and open squares for liquid samples) showing the column composition trajectories for the water (1)–ethanol (2)–cyclohexane (3) system. Also shown are the simulation results showing the trajectories calculated by the EQ stage model and the NEQ stage model. The large open circles represent the experimental composition specified in the simulations. In the NEQ model simulations a bubble size $d_b = 2.5$ mm was chosen.

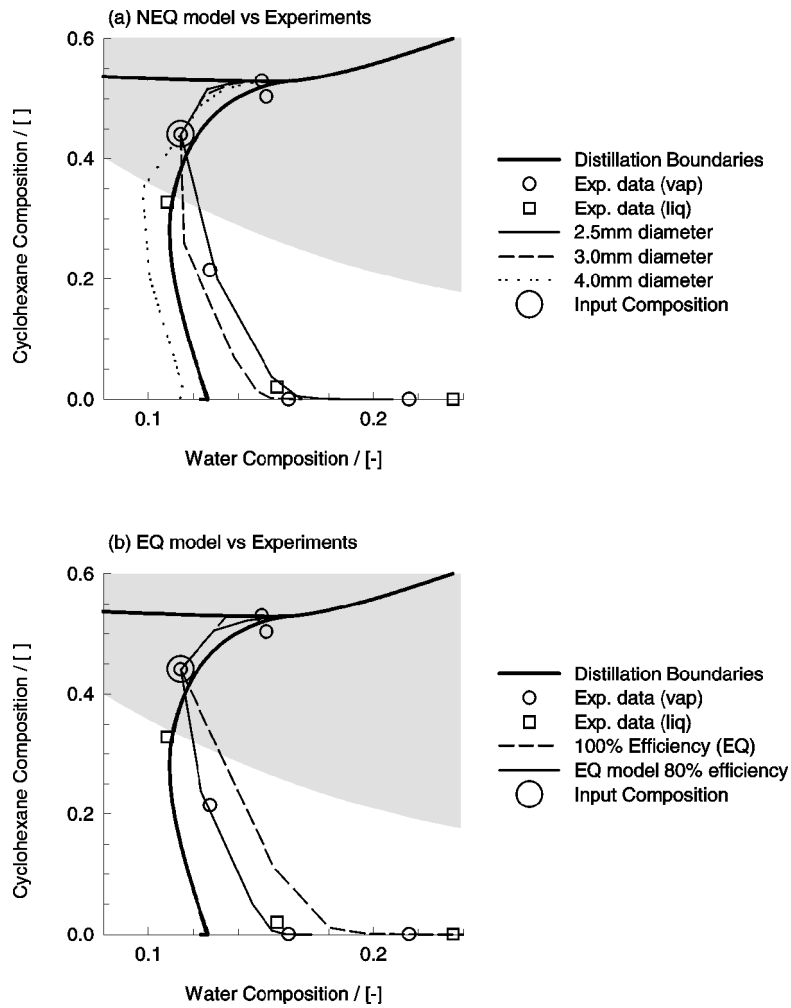

Figure 12. Simulation results compared with the experimental data (open circles for vapour samples and open squares for liquid samples) for run WEC-12 of campaign C. (a) The NEQ model for varying bubble diameters is compared with experimental results. The large open circle is the specified composition for the simulations. (a) Here the EQ model with 100% and 80%, based on averaged efficiency obtained from the NEQ simulation with a 2.5 mm bubble diameter, is compared with experimental results.

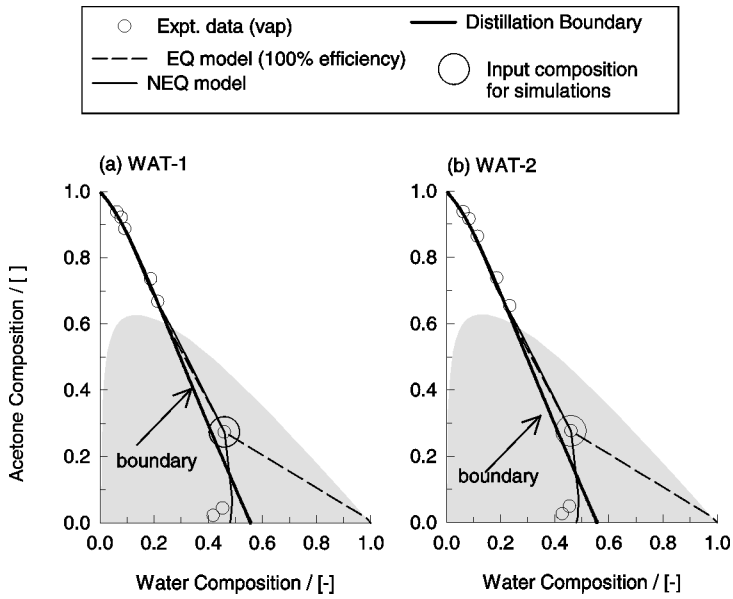

Figure 13. Experimental results showing the column composition trajectories for the water (1)–acetone (2)–toluene (3) system. Also shown are the simulation results showing the trajectories calculated by the EQ stage model (100% efficiency) and the NEQ stage model. The large open circles represent the experimental composition specified in the simulations. In the NEQ model simulations a bubble size $d_b = 2.5\,mm$ was chosen. The grey shaded areas represent the region in which liquid–liquid phase splitting occurs.

and 12), the distillation boundary is crossed. Both the EQ model (with equal component efficiencies for all components) and the NEQ model predict this boundary crossing effect. For the experiments in campaign C, the EQ model is sufficient to model the experimental results; this conclusion is in conformity with that reached by Müller *et al.* (1997).

(3) For the experimental runs in campaign B with the system water–ethanol–cyclohexane system (see Figures 8 and 9), the distillation boundary is not crossed while the EQ model anticipates boundary crossing. The NEQ model correctly predicts no boundary crossing for this campaign. These results clearly show that an EQ model, with equal component efficiencies for all components, is unable to even qualitatively explain the experimental trajectories. Our results contradict the conclusion drawn by Müller *et al.* (1997). It appears that the conclusion of Müller *et al.* (1997) that the EQ model, with equal component efficiencies, is sufficient to describe the column composition trajectories is not of general validity but applies only in restricted regions of the composition space.

(4) For the water–acetone–toluene system, the experimental results show the phenomena of boundary crossing; see Figure 13. This boundary crossing is anticipated by the NEQ model but not by the EQ model. This result is in agreement with the earlier findings of Springer *et al.* (2002a–c) for homogenous azeotropic distillation.

The overall conclusion to be drawn from this work is that, for reliable simulation of heterogeneous azeotropic distillation systems, we must adopt a rigorous NEQ stage model.

NOMENCLATURE

a_b	vapour–liquid interfacial area per unit volume of dispersion, $m^2 m^{-3}$
a_d	liquid-liquid interfacial area per unit volume of dispersion, $m^2 m^{-3}$
B_{ij}	NRTL parameters; see Table 1, K
c_i	molar concentration of species i, $mol\,m^{-3}$
c_t	mixture molar density, $mol\,m^{-3}$
d_b	bubble diameter, m
d_d	droplet diameter, m
$Đ_{ij}$	Maxwell–Stefan diffusivity for pair i–j, $m^2 s^{-1}$
E_i	component Murphree stage efficiency
G_{ij}	NRTL parameters; see Table 1
g	acceleration due to gravity, $m\,s^{-2}$
h	distance along froth height, m
h_f	height of dispersion, m
k_{ij}	element for matrix of multicomponent mass transfer coefficient, $m\,s^{-1}$
$[k]$	matrix of multicomponent mass transfer coefficients, $m\,s^{-1}$
$[K_{oG}]$	diagonal matrix of K-values
$[K^{OV}]$	matrix of multicomponent overall mass transfer coefficients, $m\,s^{-1}$
$[NTU^{OV}]$	matrix of overall number of vapour phase transfer units
n	number of species in the mixture
S	parameter defined in equation (10), $m\,s^{-1}$
Sh	Sherwood number
t_b	liquid–bubble contact time, s
T	temperature, K
V_b	single bubble rise velocity, $m\,s^{-1}$
x_i	liquid composition for component i, dimensionless
y_i	vapour composition for component i, dimensionless

Greek symbols

α_{ij}	non-randomness parameter in NRTL equation, see Table 1
ε_G	holdup of vapour
ε_d	holdup of drops
κ_{ij}	binary Maxwell–Stefan mass transfer coefficients, $m\,s^{-1}$
ρ_L	density of the liquid, $kg\,m^{-3}$
μ_L	liquid viscosity, Pa s
μ_i	molar chemical potential, $J\,mol^{-1}$
σ	surface tension, $N\,m^{-1}$
τ^V	vapour phase residence time, s

τ_{ij}	NRTL parameters; see Table 1
ξ	dimensionless distance along dispersion or column height

Subscripts

b	referring to a bubble
f	referring to the froth
i	component index
j	stage index
OV	overall parameter referred to the vapour phase
ref	reference
Lc	referring to the continuous liquid phase
Ld	referring to the dispersed liquid phase
V	referring to the y phase (vapour)

Superscripts

Lc	referring to the continuous liquid phase
Lc,b	referring to the continuous liquid phase next to bubble
Lc,d	referring to the continuous liquid phase next to drop
Ld	referring to dispersed liquid droplet phase
V	referring to the vapour phase
*	referring to equilibrium state

REFERENCES

Baur, R., Taylor, R. Krishna, R. and Copati, J.A., 1999, Influence of mass transfer in distillation of mixtures with a distillation boundary, *Trans IChemE, Part A, Chem Eng Res Des*, 77: 561–565.

Block, U. and Hegner, B., 1976, Development and application of a simulation model for three-phase distillation, *AIChE J*, 22: 582–589.

Cairns, B.P. and Furzer, I.A., 1990a, Multicomponent 3-phase azeotropic distillation. 1. Extensive experimental-data and simulation results, *Ind Eng Chem Res*, 29: 1349–1363.

Cairns, B.P. and Furzer, I.A., 1990b, Multicomponent 3-phase azeotropic distillation. 2. Phase-stability and phase-splitting algorithms, *Ind Eng Chem Res*, 29: 1364–1382.

Cairns, B.P. and Furzer, I.A., 1990c, Multicomponent 3-phase azeotropic distillation. 3. Modern thermodynamic models and multiple solutions, *Ind Eng Chem Res*, 29: 1383–1395.

Doherty, M.F. and Malone, M.F. 2001, *Conceptual Design of Distillation Systems* (McGraw-Hill, New York, USA).

Eckert, E. and Vanek, T., 2001, Some aspects of rate-based modelling and simulation of three-phase distillation columns, *Comput Chem Eng*, 25: 603–612.

Gmehling, J. and Onken, U., 1977, *Vapour-Liquid Equilibrium Data Collection* (Dechema, Frankfurt, Germany).

Kooijman, H.A. and Taylor, R., 1995, Modeling mass-transfer in multicomponent distillation, *Chem Eng J*, 57: 177–188.

Kooijman, H.A. and Taylor, R., 2001, *The ChemSep Book* (Books on Demand, Norderstedt).

Krishna, R. and Wesselingh, J.A., 1997, The Maxwell–Stefan approach to mass transfer, *Chem Eng Sci*, 52: 861–911.

Krishna, R., Urseanu, M.I., van Baten, J.M. and Ellenberger, J., 1999, Wall effects on the rise of single gas bubbles in liquids, *Int Commun Heat Mass Transf*, 26: 781–790.

Krishnamurthy, R. and Taylor, R., 1985b, A nonequilibrium stage model of multicomponent separation processes. Part I: model description and method of solution, *AIChE J*, 31: 449–456.

Krishnamurthy, R. and Taylor, R., 1985a, A nonequilibrium stage model of multicomponent separation processes. Part II: comparison with experiment, *AIChE J*, 31: 456–465.

Krishnamurthy, R. and Taylor, R., 1985c, A nonequilibrium stage model of multicomponent separation processes. Part III: the influence of unequal component efficiencies in process design problems, *AIChE J*, 31: 1973–1985.

Levy, S.G., Van Dongen, D.B. and Doherty, M.F., 1985, Design and synthesis of homogeneous azeotropic distillation. 2. Minimum reflux calculations for nonideal and azeotropic columns, *Ind Eng Chem Fund*, 24: 463–474.

Lewis, W.K. and Chang, K.C., 1928, Distillation. III. The mechanism of rectification, *Trans Am Inst Chem Eng*, 21: 127–138.

Mehlhorn, A., Espuna, A., Bonsfills, A., Gorak, A. and Puigjaner, L., 1996, Modeling and experimental validation of both mass transfer and tray hydraulics in batch distillation, *Comput Chem Eng*, 20: S575–S580.

Mendelson, H.D., 1967, The prediction of bubble terminal velocities from wave theory, *AIChE J*, 13: 250–253.

Müller, D. and Marquardt, W., 1997, Experimental verification of multiple steady states in heterogeneous azeotropic distillation, *Ind Eng Chem Res*, 36: 5410–5418.

Müller, D., Marquardt, W., Hauschild, T., Ronge, G., and Steude, H., 1997, *Experimental Validation of an Equilibrium Stage Model for Three-phase Distillation* (Maastricht, The Netherlands).

Murphree, E.V., 1925, Rectifying column calculations with particular reference to n-component mixtures, *Ind Eng Chem*, 17: 747–750.

Poling, B.E., Prausnitz, J.M. and O'Connell, J.P., 2000, *The Properties of Gases and Liquids* (McGraw-Hill, New York, USA).

Ross, B.A. and Seider, W.D., 1981, Simulation of three-phase distillation towers, *Comput Chem Eng*, 5: 7–20.

Springer, P.A.M., Buttinger, B., Baur, R. and Krishna, R., 2002a, Crossing of the distillation boundary in homogeneous azeotropic distillation: influence of interphase mass transfer, *Ind Eng Chem Res*, 41: 1621–1631.

Springer, P.A.M., van der Molen, S., Baur, R. and Krishna, R., 2002b, Experimental verification of the necessity to use the Maxwell–Stefan formulation in describing trajectories during azeotropic distillation, *Chem Eng Res Des*, 80: 654–666.

Springer, P.A.M., van der Molen, S. and Krishna, R., 2002c, The need for using rigorous rate-based models for simulations of ternary azeotropic distillation, *Comput Chem Eng*, 26: 1265–1279.

Taylor, R. and Krishna, R., 1993, *Multicomponent Mass Transfer* (John Wiley, New York, USA).

Taylor, R., Kooijman, H.A. and Hung, J.S., 1994, A 2nd generation nonequilibrium model for computer-simulation of multicomponent separation processes, *Comput Chem Eng*, 18: 205–217.

Wesselingh, J.A. and Krishna, R., 2000, *Mass Transfer in Multicomponent Mixtures* (Delft University Press, Delft, The Netherlands).

ACKNOWLEDGEMENTS

The authors acknowledge a grant from the Netherlands Organization for Scientific Research (NWO), Chemical Sciences Division (CW), for investigations on three-phase distillation. The authors are grateful to R. Taylor and A.P. Higler for providing the code to perform the three-phase distillation NEQ and EQ model calculations reported in this work.

ADDRESS

Correspondence concerning this paper should be addressed to Professor R. Krishna, Department of Chemical Engineering, University of Amsterdam, Nieuwe Achtergracht 166, 1018 WV Amsterdam, The Netherlands.

E-mail: krishna@science.uva.nl

The manuscript was communicated via our International Editor for The Netherlands, Professor P. Jansens. It was received 9 September 2002 and accepted for publication after revision 7 December 2002.